Dehydration mechanism of optical clearing in tissue

Christopher G. Rylander
Virginia Tech
Department of Mechanical Engineering and School of Biomedical Engineering and Sciences (SBES)
Corporate Research Center, RB 15, MC 0493
1880 Pratt Drive
Blacksburg, Virginia 24061
E-mail: cgr@vt.edu

Oliver F. Stumpp
Thomas E. Milner
Nate J. Kemp
The University of Texas at Austin
Department of Biomedical Engineering
1 Texas Longhorns #C0800
Austin, Texas 78712

John M. Mendenhall
The University of Texas at Austin
Institute for Cellular and Molecular Biology
Austin, Texas 78712

Kenneth R. Diller
A. J. Welch
The University of Texas at Austin
Department of Biomedical Engineering
1 Texas Longhorns #C0800
Austin, Texas 78712

Abstract. Previous studies identified various mechanisms of light scattering reduction in tissue induced by chemical agents. Our results suggest that dehydration is an important mechanism of optical clearing in collagenous and cellular tissue. Photographic and optical coherence tomography images indicate that air-immersed skin and tendon specimens become similarly transparent to glycerol-immersed specimens. Transmission electron microscopy images reveal that dehydration causes individual scattering particles such as collagen fibrils and organelles to become more densely packed, but does not significantly alter size. A heuristic particle-interaction model predicts that the scattering particle volume fraction increase can contribute substantially to optical clearing in collagenous and cellular tissue. [DOI: 10.1117/1.2343208]

Keywords: dehydration; optical clearing; density; scattering coefficient; refractive index; cell organelle; collagen fibril; optical coherence tomography; transmission electron microscopy.

Paper 05292SSRR received Oct. 3, 2005; revised manuscript received Apr. 28, 2006; accepted for publication May 1, 2006; published online Sep. 8, 2006. This paper is a revision of a paper presented at the SPIE Conference on Optical Interactions with Tissue and Cells XVI, Jan. 2005, San Jose, California. The paper presented there appears (unrefereed) in SPIE proceedings Vol. 5695.

1 Introduction

1.1 *Tissue Optical Clearing*

The response of tissue to chemical agents such as glycerol and dimethyl sulfoxide is a reduction in light scattering and corresponding increase in optical clarity. "Tissue optical clearing" permits delivery of near-collimated light deeper into tissue, potentially improving the capabilities of various optical diagnostic and therapeutic techniques. Numerous technical publications discuss methods and applications of tissue optical clearing using chemical agents,[1–11] yet understanding of the mechanisms of clearing remains incomplete.

Three hypothesized mechanisms of light scattering reduction induced by chemical agents include (1) dehydration of tissue constituents, (2) replacement of interstitial or intracellular water with an agent that better matches the higher refractive index (n) of the proteinaceous structures, and (3) structural modification or dissociation of collagen. Although the refractive index matching mechanism (2) requires dehydration (1), this mechanism is differentiated by an additional feature: replacement of water with a chemical agent. Mechanisms 1 and 2 were first proposed by Tuchin et al.,[2] and mechanism 3 was first proposed by Yeh.[7] These and possibly other unspecified dynamic mechanisms may be working synergistically or antagonistically with different relative contributions dependent on tissue type and vitality, chemical agent, and delivery method.

Dehydration and refractive index matching of intrinsic structures may be coupled. Other researchers have suggested that dehydration can reduce scattering in soft tissue by displacing water from the space between collagen fibrils, increasing protein and sugar concentrations, and decreasing refractive index mismatch.[12–16] Such refractive index matching is due to native species and is a passive process, and we explicitly differentiate it from index matching due to exogenous chemical agents intentionally introduced into the tissue.

Motivation for this paper is twofold: (1) provide evidence that dehydration is an important mechanism of optical clearing in tissues exposed to chemical agents and (2) present an analysis of how dehydration can contribute to reduced light scattering. By comparing two methods of tissue optical clearing: air-immersion and agent-immersion, we are able to isolate and investigate the dehydration mechanism of optical clearing by chemical agents in relation to other proposed mechanisms. Optical scattering changes between native and dehydrated tissue states are measured using transmission-reflection photography and optical coherence tomography

Address all correspondence to Chris Rylander, Virginia Tech, Dept. of Mechanical Engineering and SBES, Corporate Research Center, Rb 15, MC 0493, 1880 Pratt Dr., Blacksburg, VA 24061; Tel: 540–231–3134; Fax: 540–231–0970; E-mail: cgr@vt.edu

1083-3668/2006/11(4)/041117/7/$22.00 © 2006 SPIE

(OCT). Examining changes in tissue ultrastructure using transmission electron microscopy (TEM) images and predicting modification of reduced scattering coefficient using a heuristic particle-interaction model provides a better understanding of how dehydration contributes to reduce light scattering.

1.2 *Light Scattering in Tissue*

Scattering results from the interaction of light with a material of nonisotropic refractive index. The spatial refractive index distribution of a material specifies the magnitude and direction of light scattered elastically at a given wavelength. Biological tissue, such as skin, is highly scattering to visible and near infrared light because it contains high-refractive index submicron scattering particles such as collagen fibrils ($n \sim 1.47$) and cellular organelles ($n \sim 1.39$ to 1.42) surrounded by low-refractive index fluid ($n \sim 1.35$).[17,18] Light scattering theories such as Mie and Rayleigh-Gans and computational methods such as the finite difference time domain method further support that submicron scattering particles are primarily responsible for large-angle scattering.[19–21]

Light scattering theories such as Mie and Rayleigh-Gans predict a reduced scattering cross section (σ_s' cm^2) for a single particle as a function of the scattering particle radius and refractive index, the surrounding medium refractive index, and the wavelength of light in vacuum.[1,22] For a dense distribution of scattering particles, the reduced scattering coefficient (μ_s' cm^{-1}) is related to the reduced scattering cross section by a simple heuristic particle-interaction model:[1,23]

$$\mu_s' = \frac{\phi(1-\phi)}{V}\sigma_s', \tag{1}$$

where ϕ is volume fraction of scattering particles and V is the volume of a single scattering particle. Parabolic dependence on ϕ was first introduced by Twersky[24] and ensures the reduced scattering coefficient is zero in the limit of null or unity volume fractions. As the fractional volume of scattering particles approaches unity, the scatterer represents less of a discontinuity in its environment. The heuristic particle-interaction model predicts that maximum scattering occurs for a scattering particle volume fraction equal to 0.5 (Fig. 1). The parabolic dependence on ϕ may be derived from a statistical average of scattering amplitudes dependent on the well-known particle pair-distribution function.[25,26] Experimental measurements from scattering of microwave and optical radiation from dense distributions of spherical particles support the heuristic particle-interaction model.[26,27]

Equation (1) is useful for examining the mechanisms of optical clearing. Chemical agents may alter the scattering properties of tissue by changing scattering particle size, shape, packing density, refractive index, and surrounding media refractive index. These parameters experience a controlled transient excursion dependent on water and agent transport kinetics. The μ_s' parabolic dependence on ϕ is useful for understanding dehydration effects that modify the scattering particle packing density. Refractive index matching and shape or structural changes to individual scattering particles affect the reduced scattering cross section (σ_s').

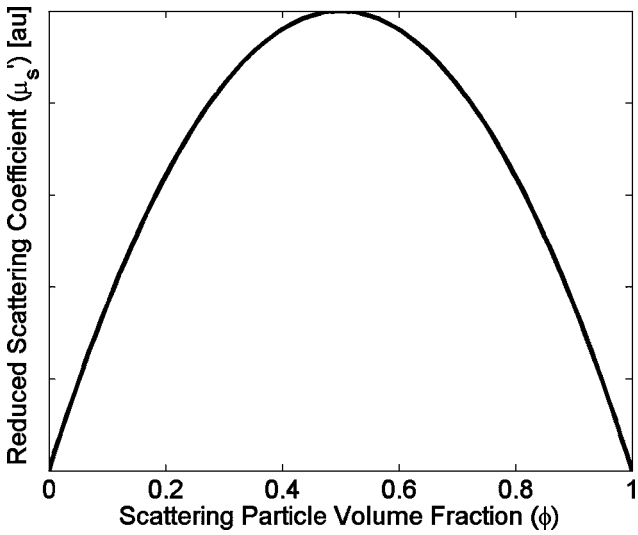

Fig. 1 Relationship between reduced scattering coefficient, μ_s', and scattering particle volume fraction, ϕ, provided r, n_{in}, n_{ex}, and λ remain constant.

2 Materials and Methods

The first aim of this paper is to provide evidence that dehydration is an important mechanism of optical clearing with chemical agents. Properties of tissue immersed in air and chemical agents are compared. The evaporative process due to air-immersion isolates the dehydration mechanism of optical clearing from other proposed mechanisms (i.e., refractive index matching by agents or structural modification of collagen). We hypothesize that if air-immersion and chemical agent-immersion induce similar optical, mass, thickness, and ultrastructural changes to tissue, then dehydration may be an important mechanism of tissue optical clearing.

Chemical agents utilized in our study include anhydrous glycerol (14.1 M) and anhydrous dimethyl sulfoxide (DMSO) (13.7 M). Air-immersion is in ambient atmosphere (approximately 25°C). Although humidity of ambient air is not controlled or recorded, it is not believed to vary greatly during sample immersion. Tissue samples included in our study are rat skin and tail tendon. Skin is a clinically relevant tissue and tail tendon is analyzed because of its known structure. Both samples are obtained from euthanized adult rats. All animals participating in this study are cared for according to Institutional Animal Care and Use Committee guidelines.

2.1 *Photographic Imaging*

Dorsal sections of full-thickness skin (approximately 4 cm^2 each) are placed in separate glass vials containing either anhydrous glycerol or DMSO. An adjacent tissue specimen is allowed to dehydrate in air. At nine time points over 100 h samples are weighed. Concurrently at these times a photographic image is recorded of each tissue sample. Each sample is positioned so that half is overlying transparent glass and half is overlying an opaque ruler that functions as a visible light transmission mask. Samples are epi- and transilluminated simultaneously with visible light and photographed using an Olympus C-3040 digital camera. Lighter regions of tissue over glass and darker regions of tissue over the opaque

ruler indicate increased transmission and decreased reflectance, respectively. The samples are otherwise kept undisturbed at room temperature.

Individual tail tendon fascicles are imaged with phase contrast microscopy (10×, Ph1 objective) in native, glycerol-immersed, and air-immersed states. The native sample is immersed in isotonic saline solution to prevent dehydration. The sample immersed in glycerol is imaged after 10 min of exposure, and the sample immersed in air is imaged after 30 min of exposure.

2.2 *OCT Imaging*

Individual tendon fascicles are imaged with an 820-nm wavelength OCT system during glycerol and air-immersion. The fascicle immersed in glycerol is imaged for 16 min, and the fascicle exposed to ambient air is imaged for 2.5 h. OCT images allow measurement of two dynamic parameters: (1) macroscopic cross-sectional diameter of the tendon fascicle and (2) depth-resolved backscattered light intensity.

2.3 *TEM Imaging of Tissue Ultrastructure*

The second aim of this paper is to detect and investigate the dehydration mechanism of optical clearing. Lateral resolution of most light-based imaging techniques are limited by diffraction and unable to reveal structural information of nanometer-sized particles responsible for light scattering. TEM, with 5-Å resolution, is capable of imaging ultrastructural changes in tissue to help understand the scattering reduction mechanisms of optical clearing. TEM is used to inspect the ultrastructure of native, glycerol-immersed and air-immersed tissue.

Specimens include rat-tail tendon fascicles and rat hepatocytes. Tendon fascicles are composed of Type I collagen, the primary constituent of human dermis. The utility of tendon as an experimental specimen is that the collagen fibrils are arranged parallel along the fascicle axis, unlike the more random fibril orientation in skin. The orderly fibril arrangement facilitates specimen orientation prior to TEM embedding and permits ultrasectioning perpendicular to the fibril axis. Hepatocytes are used in lieu of more clinically relevant epidermal keratinocytes because of the difficulty in separating them from the dermis. In addition, the liver is a homogeneous cellular structure whereas epidermis is an inhomogeneous structure composed of differentiated keratinocyte layers.

Tail tendon fascicles are cut into 2-cm-long sections and liver is cut into 1-mm^3 cubes. Both specimens are immediately submerged into anhydrous glycerol. Agent-immersed samples are extracted from respective solutions after 20 min and the excess agent is removed from the surface by placing the tissue specimens onto filter paper. The air-immersed specimens are exposed to ambient atmosphere for 2 h. All specimens, including a control, are then fixed in 5% gluteraldehyde in Hepes buffer at pH 7.2 for 1 h and later embedded in resin according to a standard protocol for TEM ultramicrotomy.[28]

Stained tissue sections are imaged with an AMT Advantage HR digital camera at magnifications of up to 28 000× on an FEI EM208 TEM at 80 kV. For consistency, images are recorded near the center of each fascicle. Cross-sectional area (and volume) fraction of the fibrils, defined as the ratio of cross-sectional area occupied by fibrils to the total image area, is quantified using a conventional thresholding image processing technique.

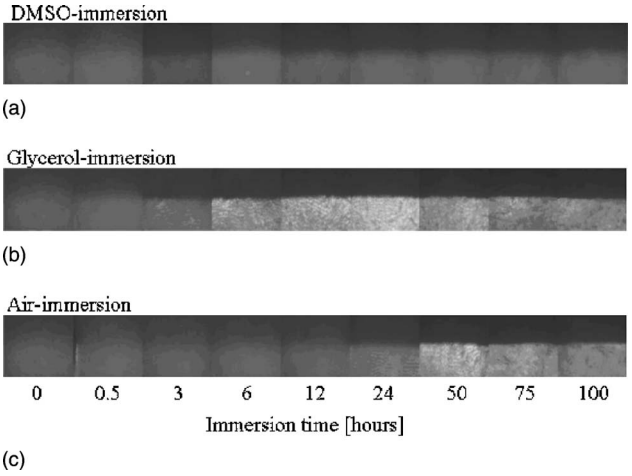

Fig. 2 Photographic images of rat skin immersed in DMSO (a), glycerol (b), and air (c). Corresponding immersion times are listed for each image.

3 Results

3.1 *Photographic Imaging*

Photographic imaging assesses optical clearing efficacy of air, glycerol, and DMSO-immersed *in vitro* rat skin. Half of each tissue specimen is placed overlying glass while the other half is placed overlying a black opaque ruler. The entire tissue specimen is simultaneously epi- and transilluminated (Fig. 2). Lighter regions of tissue overlying glass and darker regions of tissue overlying the opaque ruler indicate increased transmission and decreased reflectance, respectively. Tissue transmittance was calculated by subtracting the reflectance intensity [upper portion of Figs. 2(a)–2(c)] from the corresponding total intensity [lower portion of Figs. 2(a)–2(c)]. Reflectance from the black (highly absorbing) ruler is negligible. The ratio of transmittance to reflectance (T/R) is an indicator of scattering strength assuming absorption remains constant. A high ratio corresponds to weak scattering, while a low ratio corresponds to strong scattering.

Air-immersion past 50 h and glycerol-immersion past 24 h induce similar increases in optical clarity. Equilibrium T/R is approximately 1.5× greater for glycerol and air-immersion than DMSO-immersion. Both chemical agents increase T/R much faster than air-immersion [Fig. 3(a)]. DMSO, glycerol, and air-immersion induce 15, 40, and 55% decreases in skin mass, respectively. The decrease in skin mass is fastest for DMSO and slowest for air-immersion [Fig. 3(b)]. By nondimensionalizing with respect to time, T/R increases for increasing mass loss as shown in Fig. 3(c).

Tail tendon fascicle immersion in glycerol and air causes similar appearances when observed using phase contrast microscopy. Although the tendon fascicle immersed in glycerol optically clears more rapidly than the air-immersed specimen, at equilibrium the two tissue specimens appear similarly transparent. See Fig. 4.

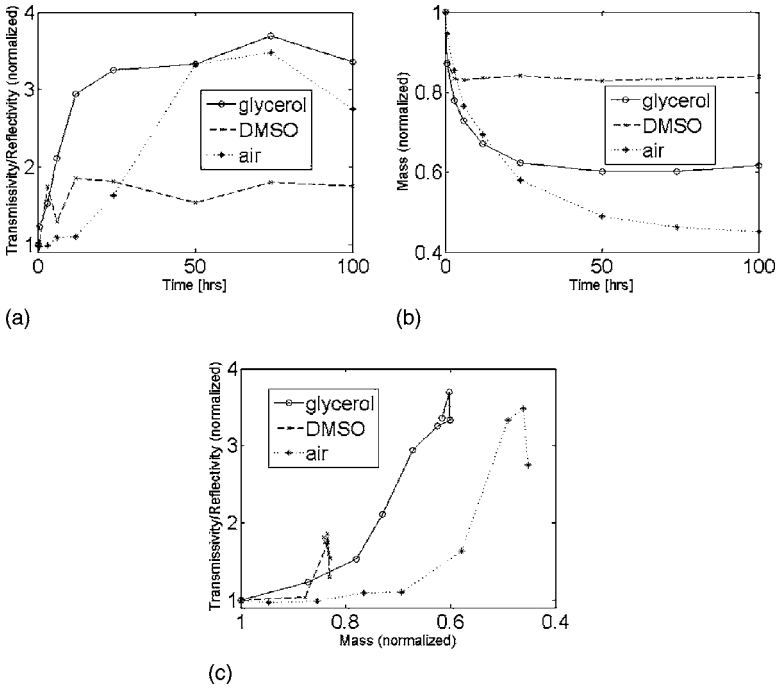

Fig. 3 (a) Normalized dynamic transmissivity/reflectivity ratio. (b) normalized dynamic skin mass. (c) normalized transmissivity/reflectivity ratio versus normalized skin mass. All plots normalize to initial values.

3.2 *OCT Imaging*

OCT M-scan images ($\lambda = 850$ nm) of tendon fascicle immersed in glycerol and air are shown in Figs. 5(a) and 5(b), respectively. A M-scan is a time sequence of depth scans into tissue at a single lateral position. The x axis of each image represents time of image acquisition, and y axis represents scan depth. Backscattered light intensity (in decibels) is plotted as a function of time and depth. Initially after exposure to glycerol or air, backscattered light from the fascicle is large because the specimen is highly turbid. At early times, effect of multiply scattered light is evident from M-scan images. Multiply scattered photons undergo a longer optical path length than single-scattered photons and artifactually appear as backscattering from beneath the fascicle.

Glycerol- and air-immersion induce similar responses in fascicle size and scattering, although the response due to glycerol is approximately an order of magnitude faster. The time constants for fascicle shrinkage and scattering reduction due to glycerol and air exposure are approximately 2 min and 20 min, respectively. Tendon fascicle scattering changes were indicated by the percentage of backscattered light intensity integrated over the fascicle thickness. Interestingly, with either glycerol- or air-immersion, scattering first increases slightly and then exponentially decays to near 5% of its original value [Figs. 5(c) and 5(d)].

Fascicle optical thickness exponentially drops 25% of its original value in response to both glycerol and air exposure [Figs. 5(e) and 5(f)]. In the case of both glycerol- and air-immersion, the average refractive index is expected to increase by a small percentage. For example, assuming complete replacement of all water within the tendon fascicle ($\sim 50\%$) with either glycerol or proteinaceous fibrils ($n = 1.47$), the average fascicle refractive index would increase 4%. The measured decrease in fascicle optical thickness of 25% may result from either a 25% decrease in physical diameter assuming no change in refractive index or approximately 29% decrease in physical thickness in combination with a 4% increase in refractive index.

3.3 *TEM Imaging of Tissue Ultrastructure*

TEM images of collagen fibril distribution are shown in Fig. 6 corresponding to (a) the native state, (b) 5-min anhydrous

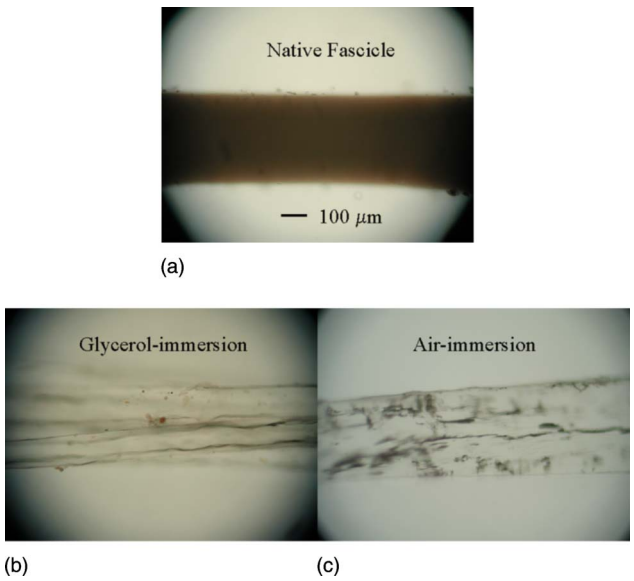

Fig. 4 Phase contrast images of tail tendon fascicle. (a) Native state. (b) 10-min glycerol-immersion. (c) 30 min air-immersion.

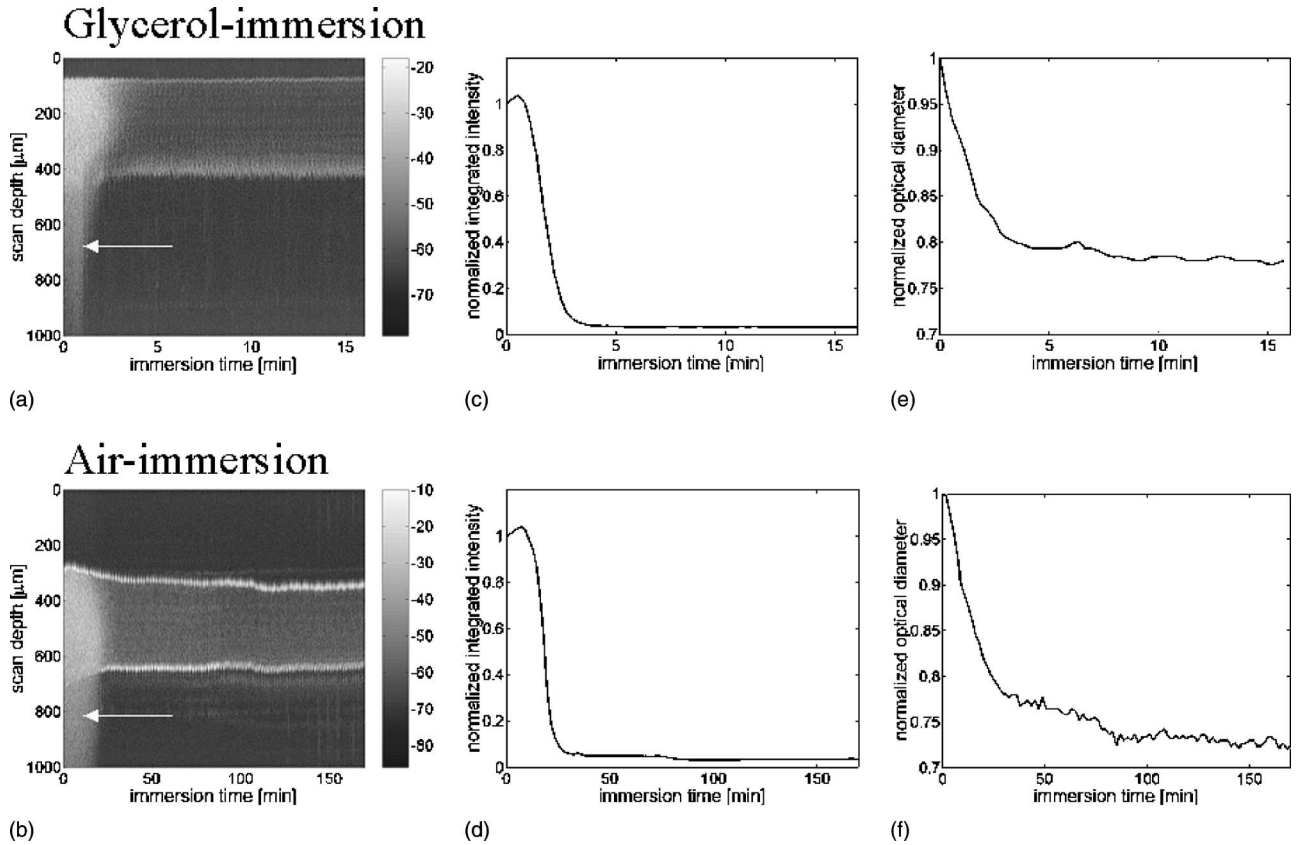

Fig. 5 OCT M-scan images (in decibels) of tail tendon fascicles immersed in glycerol (a) and air (b). Arrows indicate multiple light scattering. Normalized back-reflected light intensity integrated over fascicle diameter during immersion in glycerol (c) and air (d). Normalized fascicle optical thickness (diameter) during immersion in glycerol (e) and air (f).

glycerol-immersion, and (c) 2-h air-immersion. The largest (approximately 200-nm diameter) fibrils account for the majority of total fibril area fraction. Fibril diameter and shape do not appear significantly altered due to air-immersion; however, degraded image contrast of the glycerol-immersed specimen may be attributed to changes in fibril size and shape.

Images reveal higher fibril packing density in the glycerol- and air-immersed state versus the native state. Volume fraction of tendon fibrils increased from approximately 0.65 to approximately 0.90 due to glycerol- and air-immersion. Measured increase in scattering particle volume fraction (ϕ) corresponds to an approximately 60% decrease in reduced scattering coefficient assuming no change in refractive index ratio between fibrils and surrounding fluid or change in scattering particle size or shape [Eq. (1), Fig. 1].

TEM images of rat hepatocytes are shown in Fig. 7 corresponding to (a) the native state, (b) 10-min glycerol-immersion, and (c) 2-h air-immersion. Images reveal higher intracellular organelle volume fraction in glycerol- and air-immersed states versus the native state. Organelle area fraction is not quantitatively analyzed.

4 Discussion

Tissue dehydration is highly correlated with mass loss due to evaporation. The primary constituents of skin are water (70%

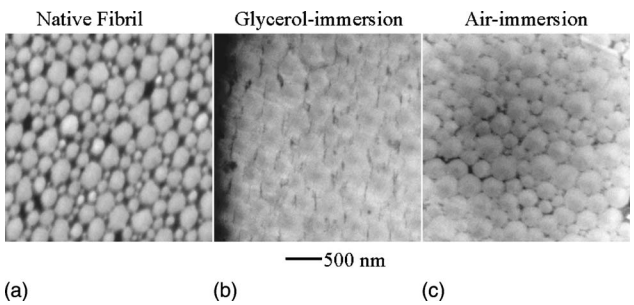

Fig. 6 TEM images of tail tendon fibrils. (a) native state. (b) 20-min glycerol-immersion. (c) 2-h air-immersion.

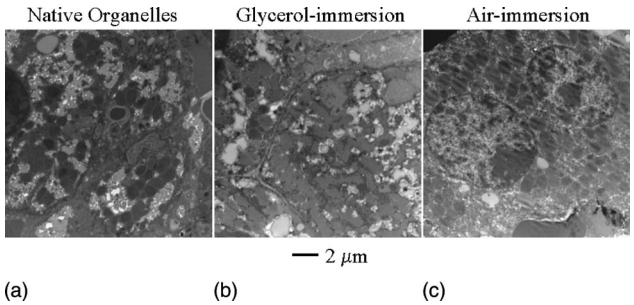

Fig. 7 TEM images of rat hepatocyte organelles. (a) native state. (b) 20-min glycerol-immersion. (c) 2-h air-immersion.

by mass) and protein (30% by mass). Of these two primary constituents, only water is volatile—it may evaporate and leave the tissue specimen at standard atmospheric temperature and pressure. Proteins (primarily collagen and proteoglycans) are nonvolatile at atmospheric pressures and physiological temperatures. In the case of agent-immersion, mass measurements cannot distinguish between water loss and agent uptake; however, because we observed a monotonic decrease in mass of DMSO and glycerol-immersed samples, we concluded that a net mass flow of liquid out of the tissue occurred in each case. Moreover, because the density of DMSO (1.1 g/cm^3) and glycerol (1.26 g/cm^3) is greater than water (1.0 g/cm^3), the measured mass decrease is a conservative estimate of the volume decrease. Taken together, our experimental results suggest that water loss or dehydration occurred in air-, glycerol-, and DMSO-immersed specimens.

Tissue optical clarity is inversely related to its state of hydration (represented by mass and thickness, Figs. 3 and 5, respectively). These results agree well with Xu and Wang's correlation between water loss and clearing capability of agents on porcine muscle and stomach.[8,9] Dehydration by air immersion produces optical property modification and ultrastructural change similar to that observed with glycerol, and therefore, we believe that glycerol may function to optically clear tissue *in-part* by the mechanism of dehydration. Photographic images indicate that air- and glycerol-immersed skin and tendon specimens become similarly transparent (Figs. 2 to 4). Similarly, OCT images indicate that rat-tail tendon fascicle thickness and integrated backscattered intensity decreased the same amount whether dehydrated in air or immersed in glycerol (Fig. 5). Because the OCT depth-resolved scattering profile indicates an intrinsic reduction in backscattered intensity, and the 95% reduction of integrated backscattered intensity over the fascicle cannot be entirely accounted for by the 25 to 30% decrease in fascicle diameter, we conclude that in air-immersed specimens, dehydration decreases the scattering attenuation coefficient. Optical clearing of DMSO- and glycerol-immersed specimens may involve multiple mechanisms, and additional studies are required to clarify the time course of action for each candidate.

We believe optical clearing mechanisms of glycerol- and DMSO-immersion may be quite different due to differences in the mass transport process. Glycerol and other hydrophilic sugar alcohols, such as mannitol and polyethylene glycol, dehydrate skin effectively because their permeabilities are 10 to 100 times less than that of water.[29] Dehydration by topical application of glycerol on *in vitro* skin may be an important mechanism of optical clearing. DMSO, however, is a well-known skin penetration enhancer and its permeability rate is approximately 10 times greater than that of water.[30] DMSO induces a reversible conformational change of protein when it substitutes for water.[9,31] Refractive index matching due to water replacement by DMSO and shape or structural modification of individual scattering particles may be important mechanisms of optical clearing for topical application of DMSO.

Mixtures of DMSO and glycerol have shown improvement in optical clearing capability, and this effect has been attributed to the membrane permeability and glycerol carrier characteristics of DMSO.[9] The synergistic effect of DMSO and glycerol may also be attributed to the combination of their aforementioned respective optical clearing mechanisms. Specifically, DMSO may function to disrupt the stratum corneum mass transport barrier, increasing water and glycerol permeability. Dehydration and optical clearing induced by glycerol may occur more quickly as a result of greater water permeability.

We believe dehydration can reduce light scattering by (1) increasing the volume fraction of scattering particles and (2) intrinsic refractive index matching due to increase of proteoglycan concentration in a ground substance.[12–16] TEM images reveal that dehydration causes collagen fibrils and organelles to become more closely packed, but does not cause a significant change in their size. Because the native tissue packing density of tendon collagen fibrils is near 65% and increases to near 90% due to dehydration, a heuristic particle-interaction model predicts that this ultrastructural change contributes to a 60% decrease in the reduced scattering coefficient, assuming no change in refractive index of the ground substance.

We believe that intrinsic refractive index matching may also contribute to optical clearing. Vargas et al. measured approximately 50% decrease in reduced scattering coefficient for 20-min glycerol-immersion of *in vitro* rat skin over visible and near infrared wavelengths.[3] Choi et al. reported approximately 67 and 33% decreases in the reduced scattering coefficient of *in vitro* human skin at 633 nm for 20-min glycerol- and DMSO-immersion, respectively.[11] Because water loss and scattering reduction have not reached a steady state at 20-min of chemical agent immersion (Figs. 2 and 3), the scattering coefficient will likely decrease further than 50% at equilibrium—an effect that cannot be solely explained by the increased volume fraction of scattering particles. The role of intrinsic refractive index matching requires further investigation of ground substance proteoglycan permeability and dependence on the state of tissue hydration.

TEM images of rat-tail tendon immersed in glycerol exhibit lower contrast than air-immersed specimens. One explanation for this observation is an artifact induced by slightly thicker tissue sections or less absorption of uranyl acetate stain. Alternatively, the effect may be attributed to a greater degree of refractive index matching between fibrils and intrafibrillar space caused by increased concentration of intrinsic proteoglycans or exogenous glycerol. In addition, alteration of fibril form and diameter may be attributed to collagen molecule disassociation as suggested by Yeh.[7]

5 Conclusions

Over the last decade, many studies have reported on both mechanisms and techniques for optical clearing of tissue using chemical agents. Numerous variations in tissue type and vitality (*in vivo* versus *in vitro*), chemical agent, and delivery method have been reported in these studies. Dynamic processes that have been cited include agent transport, water transport (dehydration), and chemical reaction. Each dynamic process can alter tissue scattering strength through modification of scattering particle packing density and distribution, scattering particle shape and size, and relative refractive index of scattering particles to the surrounding medium. Moreover, the dynamic processes can be interdependent and their relative contribution to optical clearing in specific tissues is not

well understood. Unfortunately, a primary mechanism of optical clearing that is universally applicable in all tissues for any chemical agent regardless of delivery may not exist. Based on the experimental results presented here in the context of *in vitro* rodent skin and tendon using the topical delivery of glycerol, we conclude water transport (dehydration) is an important mechanism and should be carefully considered in future studies of the optical clearing of tissues.

Acknowledgments

This research was funded by NSF Grant No. BES9986296, NSF IGERT Grant No. DGE9870653, NSF Grant No. BES0529340, and the Caster Foundation.

References

1. H. Liu, B. Beauvoit, M. Kimura, and B. Chance, "Dependence of tissue optical properties on solute-induced changes in refractive index and osmolarity," *J. Biomed. Opt.* **1**(2), 200–211 (1996).
2. V. V. Tuchin, I. L. Maksimova, D. A. Zimnyakov, I. L. Kon, A. H. Mavlutov, and A. A. Mishin, "Light propagation in tissues with controlled optical properties," *J. Biomed. Opt.* **2**, 401–417 (1997).
3. G. Vargas, E. K. Chan, J. K. Barton, H. G. Rylander III, and A. J. Welch, "Use of an agent to reduce scattering in skin," *Lasers Surg. Med.* **24**, 133–141 (1999).
4. G. Vargas, K. F. Chan, S. L. Thomas, and A. J. Welch, "Use of osmotically active agents to alter optical properties of tissue: Effects on the detected fluorescence signal measured through skin," *Lasers Surg. Med.* **29**, 213–220 (2001).
5. R. K. Wang and X. Xu, "Concurrent enhancement of imaging depth and contrast for optical coherence tomography by hyperosmotic agents," *J. Opt. Soc. Am. B* **18**(7), 948–953 (2001).
6. C. G. Rylander, K. R. Diller, T. E. Milner, and A. J. Welch, "Measurement of transient glycerol concentration in individual cells using optical low coherence reflectometry," *Cryobiology* **45**(3), 237–238 (2002).
7. A. T. Yeh, B. Choi, J. S. Nelson, and B. J. Tromberg, "Reversible dissociation of collagen in tissues," *J. Invest. Dermatol.* **121**(6), 1332–1335 (2003).
8. X. Xu and R. K. Wang, "The role of water desorption on optical clearing of biotissue: Studied with near infrared reflectance spectroscopy," *Med. Phys.* **30**(6), 1246–1253 (2003).
9. X. Xu and R. K. Wang, "Synergistic effect of hyperosmotic agents of dimethyl sulfoxide and glycerol on optical clearing of gastric tissue studied with near infrared spectroscopy," *Phys. Med. Biol.* **49**, 457–468 (2004).
10. V. V. Tuchin, "Optical clearing of tissue and blood using immersion method," *J. Phys. D* **38**, 2497–2518 (2005).
11. B. Choi, L. Tsu, E. Chen, T. S. Ishak, S. M. Iskandar, S. Chess, and J. S. Nelson, "Determination of chemical agent optical clearing potential using in vitro human skin," *Lasers Surg. Med.* **36**, 72–75 (2005).
12. G. A. Askar'yan, "The increasing of laser and other radiation transport through soft turbid physical and biological media," *Sov. J. Quantum Electron.* **9**(7), 1379–1383 (1982).
13. A. P. Ivanov, S. A. Makarevich, and A. Ya. Khairulina, "Propagation of radiation in tissues and liquids with densely packed scatterers," *J. Appl. Spectrosc.* **47**, 662–668 (1988).
14. P. Rol, P. Neiderer, U. Durr, P. D. Henchoz, and F. Frankhauser, "Experimental investigation on the light scattering properties of the human sclera," *Ophthalmic Surg. Lasers* **3**, 201–212 (1990).
15. E. K. Chan, B. Sorg, D. Protsenko, M. O'Neil, M. Motamedi, and A. J. Welch, "Effects of compression on soft tissue optical properties," *IEEE J. Sel. Top. Quantum Electron.* **2**(4), 943–950 (1996).
16. V. V. Tuchin, *Tissue Optics: Light Scattering Methods and Instruments for Medical Diagnosis*, SPIE Tutorial Texts in Optical Engineering TT38, Bellingham, WA (2000).
17. A. Brunsting and P. F. Mullaney, "Differential light scattering from spherical mammalian cells," *Biophys. J.* **14**, 439–453 (1974).
18. J. M. Schmitt and G. Kumar, "Optical scattering properties of soft tissue: a discrete particle model," *Appl. Opt.* **37**(13), 2788–2797 (1998).
19. B. Beauvoit, T. Kitai, and B. Chance, "Contribution of the mitochondrial compartment to the optical properties of the rat liver: A theoretical and practical approach," *Biophys. J.* **67**, 2501–2510 (1994).
20. A. Dunn and R. Richards-Kortum, "Three-dimensional computation of light scattering from cells," *IEEE J. Sel. Top. Quantum Electron.* **2**, 898–905 (1997).
21. R. Drezek, A. Dunn, and R. Richards-Kortum, "A pulsed finite-difference time-domain method for calculating light scattering from biological cells over broad wavelength ranges," *Opt. Express* **6**, 147–152 (2000).
22. R. Graaff, J. G. Aarnoudse, J. R. Zijp, P. M. A. Sloot, F. F. M. de Mul, J. Greve, and M. H. Koelink, "Reduced light-scattering properties for mixtures of spherical particles: a simple approximation derived from Mie calculations," *Appl. Opt.* **31**(10), 1370–1376 (1992).
23. A. Ishimaru, *Wave Propagation and Scattering in Random Media*, Academic Press, San Diego (1978).
24. V. Twersky, "On scattering of waves by random distributions. II. two-space scatterer formalism," *J. Math. Phys.* **3**(4), 724–734 (1962).
25. N. G. Khlebtsov, I. L. Maksimova, V. V. Tuchin, and L. Wang, "Chapter 1: Introduction to light scattering by biological objects," in *Handbook of Optical Biomedical Diagnostics*, PM107, SPIE Press, Bellingham, WA (2002).
26. C. I. Beard, T. H. Kays, and V. Twersky, "Scattering by random distribution of spheres vs. concentration," *IEEE Trans. Antennas Propag.* **15**(1), 99–118 (1967).
27. S. Fraden and G. Maret, "Multiple light scattering from concentrated, interacting suspensions," *Phys. Rev. Lett.* **65**(4), 512–515 (1990).
28. J. Bozzola and L. Russell, *Electron Microscopy*, 2nd ed., Jones and Bartlett, Boston (1999).
29. S. Mitragotri, "Modeling skin permeability to hydrophilic and hydrophobic solutes based on four permeation pathways," *J. Controlled Release* **86**, 69–92 (2003).
30. C. Ursin, C. M. Hansen, J. W. Van Dyk, P. O. Jensen, I. J. Christensen, and J. Ebbehoej, "Permeability of commercial solvents through living human skin," *Adv. Indust. Envt. Hyg.* **56**, 651–660 (1995).
31. D. H. Rammler and A. Zaffaroni, "Biological implications of DMSO based on a review of its chemical properties," *Ann. N.Y. Acad. Sci.* **141**, 13–23 (1967).